Development of a Prototype Nickel Optic for the Constellation-X Hard X-Ray Telescope: III

S.Romaine[a], S.Basso[b], R.J.Bruni[a], W.Burkert[f], O.Citterio[b], G.Conti[h], D.Engelhaupt[e], M.Freyberg[f], M.Ghigo[b], P.Gorenstein[a], M.Gubarev[d], G. Hartner[f], F. Mazzoleni[b], S.O'Dell[c], G.Pareschi[b], B.D.Ramsey[c], C.Speegle[g], D.Spiga[b]

[a]Harvard-Smithsonian Center for Astrophysics, Cambridge, MA 02138
[b]Istituto Nazionale di AstroFisica-Osservatorio Astronomico di Brera - 23808 Merate(Lc) - Italy
[c]Space Science Department,NASA/Marshall Space Flight Center
[d]Universities Space Research Association, Alabama
[e]Center for Applied Optics, University of Alabama in Huntsville
[f]Max-Planck-Institut für extraterrestrische Physik, Panter, Neuried, Germany
[g]Raytheon-ITSS, Alabama
[h]IASF-Sez. Milano - Italy

ABSTRACT

The Constellation-X (Con-X) mission[1] planned for launch in 2015, will feature an array of Hard X-ray telescopes (HXT) with a total collecting area greater than 1500 cm^2 at 40 keV. Two technologies are being investigated for the optics of these telescopes, including multilayer coated Electroformed-Nickel-Replicated (ENR) shells. The attraction of the ENR process is that the resulting full-shell optics are inherently stable and offer the prospect of better angular resolution which results in lower background and higher instrument sensitivity. We are building a prototype HXT mirror module using an ENR process to fabricate the individual shells. This prototype consists of 5 shells with diameters ranging from 150 mm to 280 mm with a length of 426 mm. The innermost of these will be coated with iridium, while the remainder will be coated with graded d-spaced W/Si multilayers. Parts I and II of this work were presented at the SPIE meetings in 2003 and 2004. This paper presents a progress update and focuses on accomplishments during this past year. In particular, we will present results from full illumination X-ray tests of multilayer coated shells, taken at the MPE-Panter X-ray facility.

Keywords: X-ray Telescopes, X-ray optics, multilayers, electroformed optics

Corresponding author: S. Romaine, email: sromaine@cfa.harvard.edu

Optics for EUV, X-Ray, and Gamma-Ray Astronomy II, edited by Oberto Citterio, Stephen L. O'Dell,
Proc. of SPIE Vol. 5900, 59000S, (2005) · 0277-786X/05/$15 · doi: 10.1117/12.620438

1. INTRODUCTION

We are fabricating a prototype optic for the hard X-ray telescope of Constellation-X. The approach we are taking is to use electroformed nickel replicated shells, similar technology to that of JET-X/SWIFT and XMM/Newto

The use of full-shell optics which are inherently stable, offers the prospect of better angular resolution and therefore lower background and higher instrument sensitivity.[2] However, it is necessary to develop the technology beyond that of JET-X to produce shells that will meet the mass limit, effective area and larger bandwidth planned for Con-X. In particular, the wall thickness of the shells developed for Con-X must be a factor of $\approx$ three thinner than that of JET-X, the shells must be coated with multilayers to meet the higher bandwidth and the focal length must be three times longer than that of JET-X.

As discussed below, INAF-OAB (Instituto Nazionale di AstroFisica-Osservatorio Astronomico di Brera) and MSFC (Marshall Space Flight Center) are both developing technologies to produce shells that meet the necessary requirements.[3,4] The multilayer coating is being carried out at Smithsonian Astrophysical Observatory (SAO) and MPE-Panter Facility is being used to collect full illumination high energy data of prototype shells.

2. MULTILAYER COATING FACILITY AT SAO

Figure 1 presents a photograph of the multilayer coating chamber at SAO. Multilayer coating tests were completed on witness samples while the process was being developed and results of these tests were discussed in earlier papers.[5–7]

The focus now is on the coating of complete shells. The shells produced by MSFC and INAF-OAB differ slightly in the bulk material (NiCo vs. Ni) and in the material left on the inside surface of the shell after replication (Ni oxide vs. gold). Work is now underway to understand variations that may arise when depositing muiltilayers on these two different surfaces/materials.

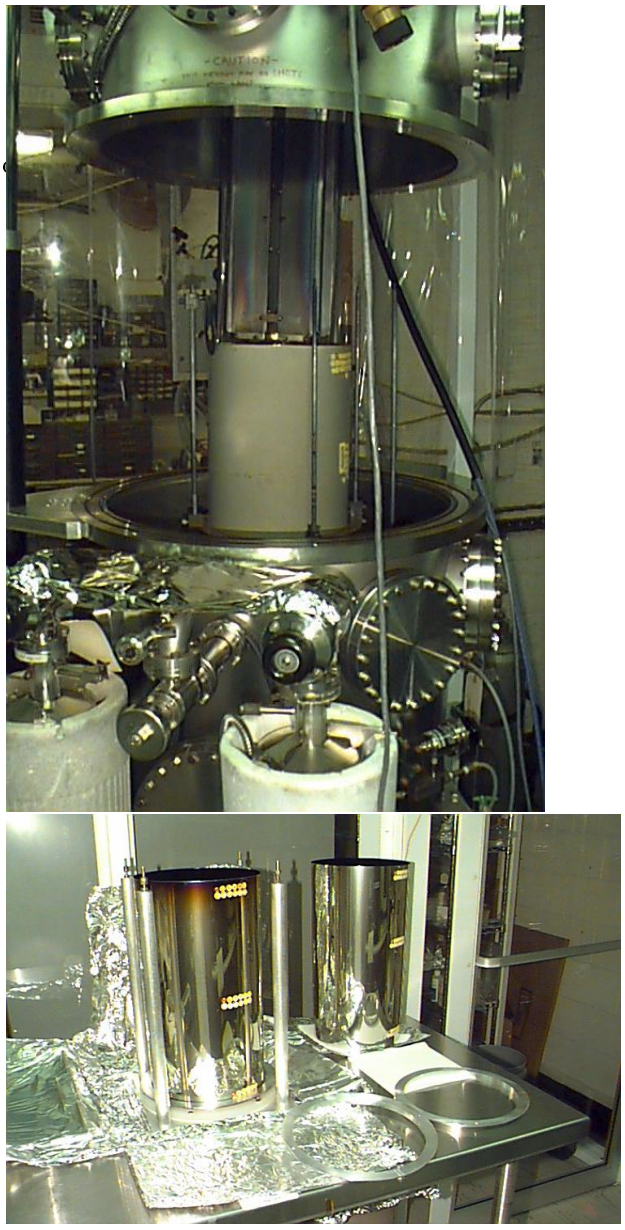

Figure 1. Top photo shows SAO DC magnetron coating chamber with INAF-OAB shell, 200 microns thick, 60 cm long, 30 cm diameter. Bottom photo: MSFC coated shells 42.6 cm long, 23 cm diameter, shell on left 100 microns thick, shell on right 150 microns thick.

3. THE PROTOTYPE

Figure 2 is a sketch of the prototype that is being fabricated, and shows the mirror shells inside the spider module used for mounting/aligning. The prototype consists of 5 shells 42.6 cm long with diameters 15, 23, 25, 27 and 28 cm with a focal length of 10 meters. The inner 2 shells (and mandrels) are being fabricated at MSFC, the remaining three are being provided by INAF-OAB. The inner-most shell will be iridium coated at MSFC, the four outer shells will have W/Si multilayer coatings provided by SAO.

The spider module was fabricated at INAF-OAB and is now in use in our full beam illumination X-ray tests. During the current stage of development, the emphasis has been on the production, mounting and testing of single shell optics and the refinement of the

process using only one mandrel at each site (MSFC and INAF-OAB); the completion of the remaining mandrels will take place only after all tests have been satisfactorily completed.

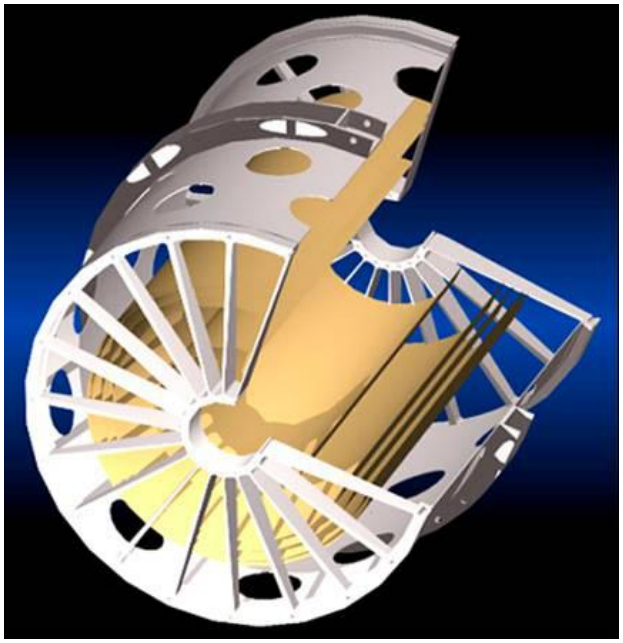

Figure 2. Drawing of spider module used for mounting/aligning shells. The 5 shells for the proposed prototype are shown. The shells will have a 10 meter focal length with diameters ranging from 15 to 30 cm and a shell length of 42.6 cm.

4. MANDREL/SHELL DEVELOPMENT

The technology being developed at MSFC is an outgrowth of a NASA SR&T program for the development of replicated optics (B. Ramsey, P.I.) and the process was initially demonstrated in the fabrication of the optics for the HERO balloon payload.[4] The mandrel diameters required for Con-X are much larger than those used for HERO and the microroughness requirement for the Con-X surfaces is much more stringent than that required for HERO. Therefore, it was necessary to develop the process at MSFC further to create larger, smoother mandrels and also to develop the separation process to produce shells with better microroughness.

The process being developed at INAF-OAB builds on the technology that was developed for JET-X and XMM which achieved better than 15 arcsec resolution. Additional obstacles must be overcome to adopt this process to the requirements of Con-X. Although the mandrel diameters produced for XMM were similar to that required for Con-X, the focal length of Con-X is almost three times that of JET-X (10 meters vs. 3.5 meters) which results in a much shallower graze angle for the mandrel/shell and therefore requires a refinement of the separation process to avoid any deformation to the final figure.

The mass limit for Con-X requires shells as thin as 100 microns which added a further constraint to both facilities (MSFC and INAF-OAB) and necessitated changes in their processes to produce these shells, while still retaining the figure and surface microroughness necessary for Con-X. MSFC has developed a process to use a NiCo alloy (instead of pure Ni) to provide higher strength and more elastic material which allows the fabrication of 100 micron thick shells while still retaining a good figure.

INAF-OAB had fabricated a 30 cm diameter, 130 μ thick shell from a JET-X mandrel. Imaging X-ray tests carried out at MPE-Panter last year yielded a measured HEW of 25 arsec, well below the 1 arcmin requirement of the HXT (O. Citterio, private communication). However, this shell had a shorter focal length than that required for Con-X and it had not been coated with multilayers.

5. X-RAY TESTING OF SHELLS AT MPE-PANTER FACILITY

The data reported in *this* paper are from the first fully-integrated MSFC NiCo replicated shell coated with W/Si multilayers. The shell was 150 microns thick, 42.6 cm long, 23 cm diameter with a 10 m focal length. The coating applied was a graded-d W/Si with N=95 as follows: the bottom N=75 bilayers were (Si=22-33 Å; W=12-17 Å) followed by a deposition of N=20 bilayers of (Si=30-100 Å; W=21-58 Å). The coating was chosen to give approximately 30% reflectivity at 20 keV, for the finite distance of the Panter source. Under these conditions the graze angle was 0.27 degrees, considerably larger than it would be for an infinite source distance.

After fabrication at MSFC, the W/Si multilayer coating was applied at SAO and the coated shell was integrated into the spider assembly using the UV vertical alignment facility at INAF-OAB. Figure 3 shows a photograph of the alignment facility which is described in detail in.[8] Full beam illumination X-ray data was then collected at MPE-Panter Facility, and the results are presented below.

5.1. The setup

The MPE-Panter X-ray Facility has been described previously in[9, 10] and we refer the reader to these papers

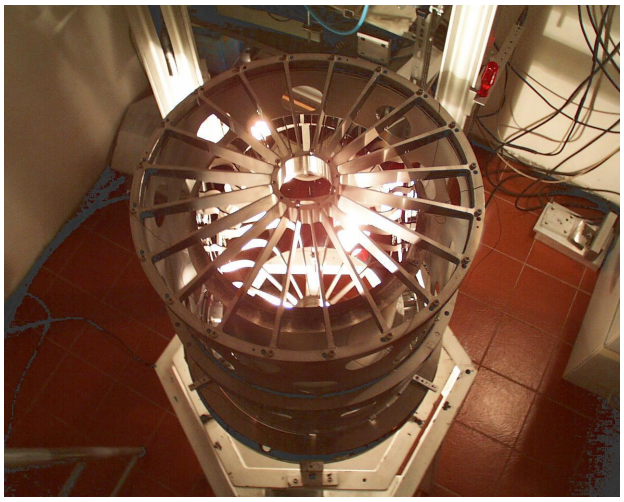

Figure 3. Spider with single shell mounted shown in UV vertical alignment Facility at INAF-OAB.

for more complete details of the facility. Here we only briefly list the setup used in our testing.

Several different anodes mounted on a target wheel were used to provide charasteristic X-ray lines from 0.28 keV to 8.05 keV. Coupled with a ROSAT type PSPC detector, this combination is useful for measuring encircled energy and HEW. In addition, a sealed source tungsten anode with a 60 kV supply can be used to provide a source of photons with energy range 4.5 to 50 keV, using the bremsstrahlung continuum component of the energy spectrum. An XMM type pn-CCD detector was used with the tungsten anode source to measure reflectivity and effective area. The measurements were taken in energy dispersive mode, with a broad beam illuminating the full optic.

Figure 4 is a photograph of the spider module and shell in the X-Ray pipe. The module is shown fixtured to the Panter manipulator mounted at the entrance to the testing chamber. X-rays travelling down the pipe reflect off the optic and are focused on the detector mounted in the focal plane (not visible in this photo). The radial ribs that can be seen in the figure are part of the spider structure used to fixture the shell.

There are two shutters: one shutter allows X-rays to impinge only on the optic, the reflected photons being collected at the focal plane; the second shutter blocks the optic and allows photons to pass through the central opening for measuring flat-field counting rates used to monitor beam intensity and stability.

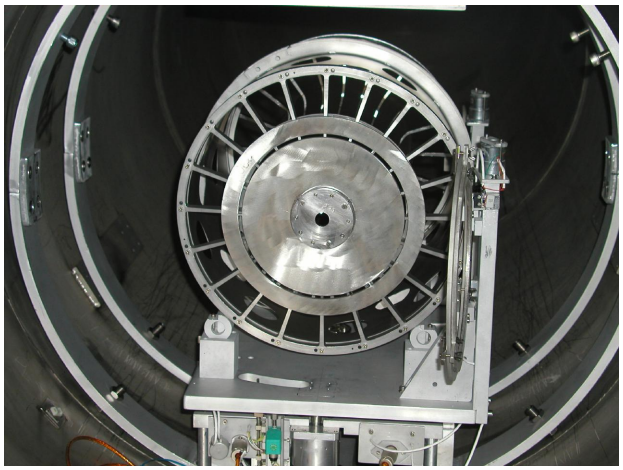

Figure 4. Photograph of spider module in Panter X-ray pipe. Shutter door can be seen open to the right of the module and the ring exposing the mirror shell is visible. The hole in the center is used for flat-field photon count rate and a second shutter exists in back of the module which can be operated to open/close this central hole.

5.2. Beam Geometry

The design of a Wolter I type optic is such that the graze angle of the parabola and hyperbola sections of the optic are equal for an infinite source distance (i.e. for incoming parallel rays), and all photons that reflect off the parabola will also reflect off the hyperbola section. However, most ground based measurements provide finite source distances with some divergence, and one must take into account the effect of the divergence of the beam when calculating the graze angles and focal length. In particular, with a 123 meter source distance of the Panter facility and an optic with : 23 cm diameter, 42.6 cm length and 10 m focal length, the beam divergence is 0.054 degrees, making a graze angle on the parabola of 0.218 degrees and on the hyperbola of 0.111 degrees.

As a result of this difference in graze angle (parabola vs. hyperbola), some of the photons that strike the front of the parabola miss the hyperbola, thereby reducing the effective area. (these 'single-bounce' photons create a ring around the periphery of the image.) The fraction of the area that contributes to the true image, i.e. that part of the optic that is involved in doubly-reflected photons, can be calculated using the equation: $afrac = (D_s - 4f)/(D_s + 4f)$, where D_s is the distance of the source from the optic and f is the focal length of the optic. For the optic discussed here, this fraction is 51%, and must be taken into account when calculating effective area. In addition, the area

vignetted by the spider arms in the module structure that holds the optic is 10%, which must also be folded into the calculation.

The collecting area of the optic (corrected for finite source distance) can be calculated using: $area = 2piR(l/2)tan(\alpha_p)$; where α_p is the graze angle for the parabola for a finite source distance, l is the length of the optic and R the radius, giving area = 5.864 cm^2 for the optic discussed here. Taking into account that fraction of the area that contributes to a single reflection only (49%) and the 10% vignetting due to the spider ribs, the corrected area = 2.69 cm^2.

5.3. The Data

The first set of data were taken at low energies using monochromatic X-ray lines from 0.27 keV to 8.05 keV and using the PSPC detector. This data provides a good measure of the quality of the figure of the shell which includes any deformation introduced by stress due to the coating, shipping or errors associated with the module mounting process. Figure 5 is a plot of the radial profiles shown as surface brightness vs. radius for five different monochromatic energy lines ranging from 0.93 to 8.05 keV. The overlap of the data shows a

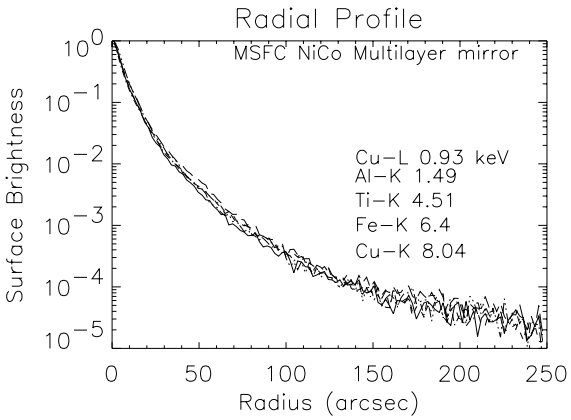

Figure 5. Surface brightness vs. Radius for several of the monochromatic lines used for testing the W/Si multilayer coated shell. The data show a smooth decrease in brightness from the peak; it's difficult to distinguish much differentiation over this energy range (0.93 to 8.05 keV).

reasonable and consistent decrease in surface brightness from the central peak out to several arcminutes radius. More interesting are the plots of *integrated* radial profiles shown in figure 6 as % encircled energy vs. radius. A section of this plot has been expanded in figure 6b to show more clearly the half energy widths. Table 1 gives the HEW for each of the monochromatic lines, showing the HEW ranges from 26.5 arcsec at the lowest energy (0.27 keV) to 30.5 arcsec at the highest energy (8.05 keV). This increase in HEW with increasing energy is due to the scattered intensity which becomes more dominant at higher energies (discussed below).

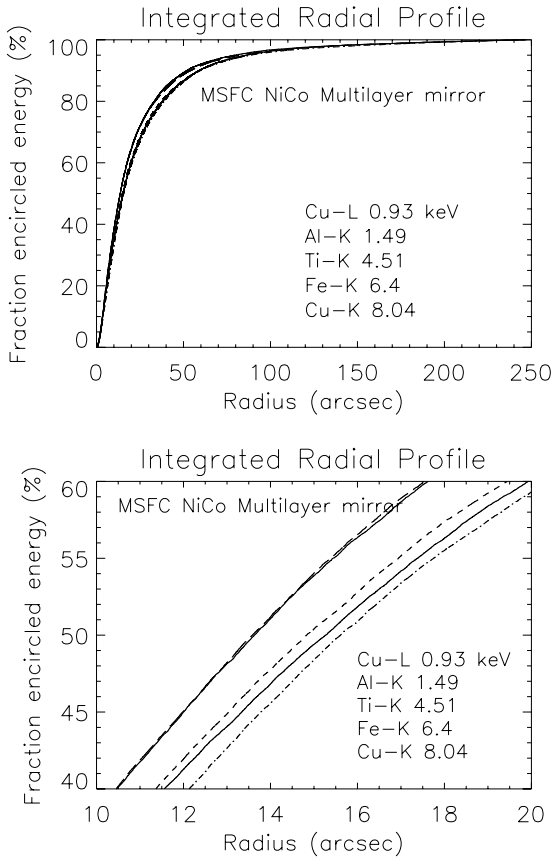

Figure 6. Fraction of encircled energy vs. Radius calculated for the monochromatic energy/PSPC data. Plot (top) shows a smooth increase in the radial profile; plot (bottom) is an expanded view of the section of the plot around the 50% encircled energy point, showing some increase in the half energy width with increasing energy. This increase is due to the microroughness which has a greater effect at higher energies (see text for more details).

The second set of data were taken using the energy dispersive setup with the pn-ccd detector and covers an energy range of $\approx$ 12 to 50 keV. Due to the limited count rate capability of the ccd, pile-up of pulses became a problem. Therefore the pn-CCD high energy data could not be used to calculate HEW. However, by de-focusing the beam, to spread the photons out over a larger area of the detector, it was possible to eliminate the pile-up and accurately measure the total reflectivity. This data is shown in figure 7 which presents a plot

Table 1. Calculated half energy widths for data shown in figure 6

Energy (keV)	HEW (arcsec)
0.27	26.5
0.93	26.5
4.51	28.5
5.41	28.5
6.40	29.0
8.05	30.5

of total reflectivity vs. energy for the pn-CCD data along with a model fit (solid line) produced using IMD software.[11] The reflectivities calculated from the low energy PSPC data have also been plotted in this same figure (using '*' symbol). A good model fit to the data was obtained using a microroughness of 10 Å, higher than that of the witness sample for this run. Figure 8, shows a plot of reflectivity vs. grazing angle for one of the witness samples coated with the shell. The witness substrate is super polished fused silica with a surface microroughness of $\leq 2\mathring{A}$, and provides a good check of the smoothness of the coating itself. The data is shown along with a good model fit which uses a microroughness of 2.8 Å. The higher microroughness modelled for the shell in figure 7 is probably due to the microroughness of the bare shell; however, due to scheduling conflicts we did not have an opportunity to measure this before coating. The polishing and separation processes are still being refined at MSFC, so we did not expect this shell to have a 5 Å surface (which is our goal). The next set of tests will include microroughness measurements on the shell before coating. If the microroughness is due to the separation, it will be necessary to add a smoothing step to the process after separation from the mandrel.

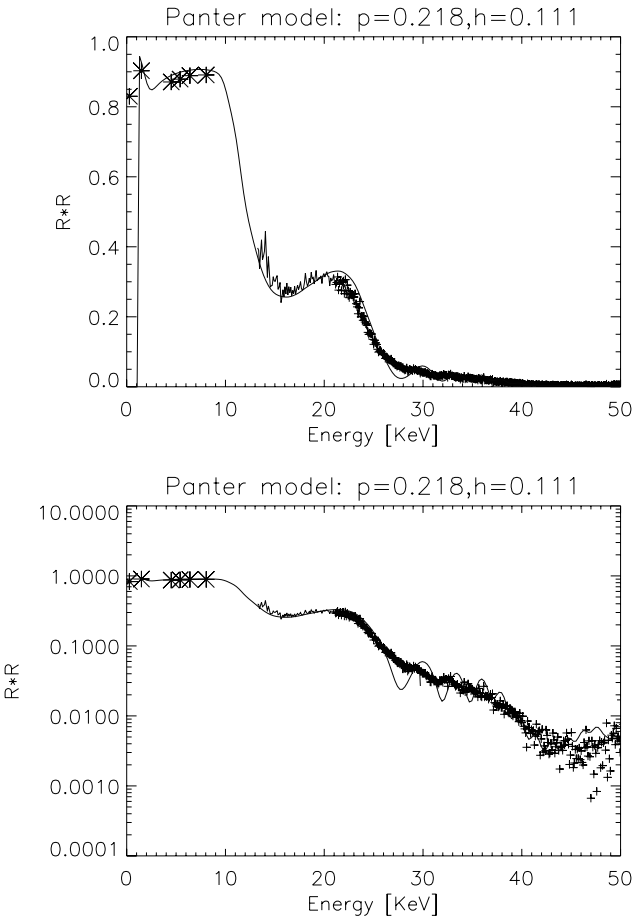

Figure 7. Plot of R(parabola)*R(hyperbola) vs. Energy; pn-ccd data taken at 30 kV and 50 kV voltage setting (shown as +) along with model fit (solid line) and PSPC data (*) for 6 discrete energies. See text for details. Linear plot (top), log plot of same data (bottom)

6. FUTURE WORK

Work is continuing to push this technology to produce ENR optics closer to our 15 arcsec goal. The 30" results reported for the MSFC NiCo optic were greater than expected, based on axial figure metrology carried out on this optic at MSFC[12, 13] which showed a 16 arcsec figure. Based on these tests, it should be possible to improve our current results and achieve our 15 arcsec goal. The high microroughness (10 Å) of the coated shell is most likely due to a 'rough' surface created when the shell separates from the mandrel. MSFC has recently purchased a moveable head AFM which will allow direct microroughness measurements to be taken of the inside surface of the shell after replication. If this is the case, further polishing of the mandrel, or cleaning of the shell can be done to improve the microroughness before coating. Upgrades in the system at MPE-Panter will be carried out to avoid pile-up issues making it possible to use high energy (10 - 50 keV) Pn-CCD measurements to calculate HEW for the high energy region.

Testing of more shells is planned to improve both processes of mandrel/shell production and to better understand the contributions of each stage of the process to the final figure of the optic.

7. SUMMARY

SAO, MSFC and INAF-OAB have collaborated to produce integral optics for the Hard X-ray telescope pro-

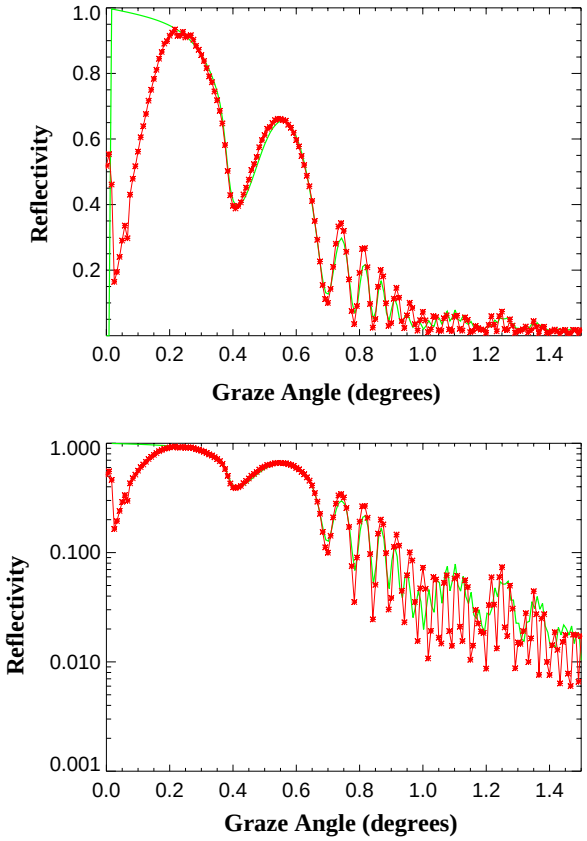

Figure 8. Plots of reflectivity vs. grazing angle for witness sample coated in chamber with optic. Data is plotted using '+' symbols, solid line is the model fit to the data. Microroughness used for this model fit is 2.8 Å. Linear plot (top), log plot (bottom).

totype for Con-X.

The electroformed nickel replicated process has been used to fabricate shells which were subsequently coated with multilayers, fitted to an engineered structure and tested with full-beam illumination X-rays at MPE-Panter Facility. Tests were carried out with energy band from $\approx$ 1 to 50 keV and using data from both PSPC and pn-ccd detectors, spatial resolution and effective areas have been calculated.

Work remains to be done to further improve both processes with a goal to produce shells with 15 arcsec figure and 5 angstroms microroughness. These will be tested at the Panter Facility.

ACKNOWLEDGMENTS

This work was supported in part by NASA contract NAG5-5354 and NASA subcontract 44A-1046805.

REFERENCES

1. J.Bookbinder et al., "The Constellation-X Mission and its Optics", *Proc. SPIE* **4496**, p.84 (2001).
2. P.Gorenstein et al., "Integral shell mirrors for the Constellation X-ray Mission Hard X-ray Telescope", *Proc. SPIE* **4138**, p.10 (2000).
3. O.Citterio et al., "Development of Soft and Hard X-ray optics for Astronomy", *Proc. SPIE* **4138**, p.43 (2000).
4. B.Ramsey et al., "The Development of Hard-X-Ray Optics at MSFC", *Proc. SPIE* **5168**, p.129, (2003).
5. A.Ivan, et al., "Influence of deposition parameters on the reflectivity of multilayer hard x-ray mirrors", *Proc. SPIE* **4501**, p.142 (2001).
6. A.Ivan et al., "Hard X-ray multilayers: a study of different material systems", *Proc. SPIE* **4145**, p.72 (2000).
7. S.Romaine, et al., "Development of a Prototype Nickel optic for the Constellation-X Hard X-Ray Telescope", *Proc. SPIE* **5168**, p.112, (2003).
8. G.Pareschi et al., "Development of grazing-incidence multilayer mirrors by direct Ni electroforming replication; a status report", *Proc. SPIE* this proceedings (2005).
9. H.Bräuninger, et al., "Calibration of hard X-ray (15-50 keV) optics at the MPE test facility Panter", *Proc. SPIE* **5168**, p.283, (2003).
10. D. Spiga, "Development of Multilayer-Coated Mirrors for Future X-Ray Telescopes", Ph.D. Thesis, Universita di Milano-Bicocca, 2005.
11. D.L.Windt, "IMD:Software for modelling the optical properties of multilayer films", *Computers in Physics*, **12** p.360 (1998).
12. M.Gubarev, et al., "Figure Measurements of High-Energy-X-Ray Replicated Optics", *Proc. SPIE* **5168**, p.227, (2003).
13. M.Gubarev et al., "Alignment,assembly,and testing of high-energy x-ray optics", *Proc. SPIE* this proceedings (2005).